

Drell-Yan Lepton-Pair-Jet Correlation in pA Collisions

Anna Staśto^{a,b,c}, Bo-Wen Xiao^a, David Zaslavsky^a

^a*Department of Physics, Pennsylvania State University, University Park, PA 16802, USA*

^bRIKEN BNL Research Center, Building 510A, Brookhaven National Laboratory, Upton, NY 11973, USA

^c*H. Niewodniczański Institute of Nuclear Physics, Polish Academy of Sciences, Kraków, Poland*

Abstract

Determining the dipole model unintegrated gluon distribution (UGD) is a problem of significant interest in small- x physics. Here we relate the dipole gluon distribution to the angular correlation function of the process $pA \rightarrow \ell \bar{\ell} \pi^0 X$, which provides a clean probe of the nuclear structure, and compute numerical predictions for the correlation function based on three models for the UGD: the GBW model, and BK evolution with fixed and running coupling. With all three models, the correlation exhibits an interesting double-peak structure, but the BK evolution is necessary to reproduce the near-side emission peak.

1. Introduction

One of the major initiatives in small- x physics is the determination of parton distributions in nucleons and nuclei. While there is already much data available on integrated quark and gluon PDFs, the unintegrated gluon distributions (UGDs) have not been so well studied, and thus determining their nature is a current focus of the small- x community. There are actually two independent UGDs: the Weizsäcker-Williams gluon distribution, which can be interpreted as the gluon number density in light-cone gauge and is probed by DIS interactions, and the dipole gluon distribution, which is instrumental in various cross-section calculations, in particular Drell-Yan processes such as what is studied here.

Our focus will be on the angular dependence of the process $pA \rightarrow \ell\bar{\ell}\pi^0 X$. Lepton pair production processes such as this one give a clean probe of the dipole gluon distribution relative to multijet events, because the virtual photon escapes from the collision without final-state interactions, and the fragmentation $\gamma \rightarrow \ell\bar{\ell}$ can be calculated exactly. This allows one to compute an exact analytical expression for the correlation $C^{\text{DY}}(\Delta\phi)$. This quantity reveals additional information about the UGD of the nuclear target as compared to the inclusive cross section alone, which has been the focus of previous studies.

This is a summary of work originally published in reference [1].

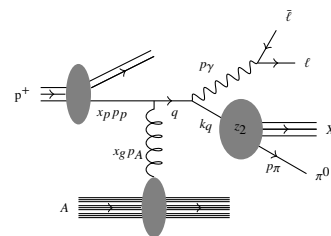


Figure 1: $pA \rightarrow \ell\bar{\ell}\pi^0 X$ at tree level with kinematic variables labeled. Adapted from reference [1].

Email addresses: astasto@phys.psu.edu (Anna Stařto), bux10@psu.edu (Bo-Wen Xiao), dzaslavs@phys.psu.edu (David Zaslavsky)

Preprint submitted to Nuclear Physics A

2. Calculation

Our analysis concerns itself with the process $pA \rightarrow \ell\bar{\ell}\pi^0 X$ at tree level, as shown in figure 1. This channel dominates the Drell-Yan lepton pair production at small x . In the figure p_p and p_A are the momenta of the proton and nucleus, x_p and x_g are the momentum fractions of the interacting quark and gluon, and $z_2 = p_\pi^+/k_q^+$ is the longitudinal momentum fraction of the quark jet which is carried by the pion. Also $z = p_\gamma^+/q^+$ (not shown in the figure) is the fraction of total momentum taken by the photon.

The exclusive cross section for this process has been explicitly calculated [2]:

$$\begin{aligned} \frac{d\sigma^{pA \rightarrow \gamma^* \pi^0 X}}{dY_\gamma dY_\pi d^2\mathbf{p}_{\gamma\perp} d^2\mathbf{p}_{\pi\perp} d^2b} &= \int_{\frac{z_2}{1-z_2}}^1 \frac{dz_2}{z_2^2} \sum_f D_{\pi^0/f}(z_2, \mu) x_p q_f(x_p, \mu) \frac{\alpha_{\text{em}} e_f^2}{2\pi^2} (1-z) F_{x_g}(q_\perp) \\ &\times \left\{ [1 + (1-z)^2] \frac{z^2 q_\perp^2}{[\tilde{P}_\perp^2 + \epsilon_M^2][(\tilde{\mathbf{P}}_\perp + z\mathbf{q}_\perp)^2 + \epsilon_M^2]} \right. \\ &\quad \left. - z^2(1-z)M^2 \left[\frac{1}{\tilde{P}_\perp^2 + \epsilon_M^2} - \frac{1}{(\tilde{\mathbf{P}}_\perp + z\mathbf{q}_\perp)^2 + \epsilon_M^2} \right] \right\}, \quad (1) \end{aligned}$$

where $\epsilon_M^2 = (1-z)M^2$ with M being the invariant mass of the virtual photon (i.e. of the lepton pair), $\mathbf{q}_\perp = \mathbf{p}_{\gamma\perp} + \mathbf{k}_{q\perp}$, and $\tilde{\mathbf{P}}_\perp = (1-z)\mathbf{p}_{\gamma\perp} - z\mathbf{k}_{q\perp}$. The gluon distribution is defined as the Fourier transform of the dipole scattering amplitude: $F_{x_g}(q_\perp) = \int \frac{d^2\mathbf{r}_\perp}{(2\pi)^2} e^{-i\mathbf{q}_\perp \cdot \mathbf{r}_\perp} S_{x_g}^{(2)}(r_\perp)$. From this we can then compute the inclusive cross section by integrating over the phase space of the quark,

$$\begin{aligned} \frac{d\sigma^{pA \rightarrow \gamma^* X}}{dY_\gamma d^2\mathbf{p}_{\gamma\perp} d^2b} &= \int_{z_{\text{hl}}}^1 \frac{dz}{z} \iint d^2\mathbf{q}_\perp \sum_f x_p q_f(x_p, \mu) \frac{\alpha_{\text{em}} e_f^2}{2\pi^2} F_{x_g}(q_\perp) \\ &\times \left\{ [1 + (1-z)^2] \frac{z^2 q_\perp^2}{[p_{\gamma\perp}^2 + \epsilon_M^2][(\mathbf{p}_{\gamma\perp} - z\mathbf{q}_\perp)^2 + \epsilon_M^2]} \right. \\ &\quad \left. - z^2(1-z)M^2 \left[\frac{1}{p_{\gamma\perp}^2 + \epsilon_M^2} - \frac{1}{(\mathbf{p}_{\gamma\perp} - z\mathbf{q}_\perp)^2 + \epsilon_M^2} \right] \right\}. \quad (2) \end{aligned}$$

The correlation function $C^{\text{DY}}(\Delta\phi)$ is the ratio of the exclusive to inclusive cross section:

$$C^{\text{DY}}(\Delta\phi) = \frac{2\pi \int \dots \int_{P_{[\gamma,\pi]\perp} > P_{\perp\text{cut}}} d\mathbf{p}_{\gamma\perp} d\mathbf{p}_{\pi\perp} \frac{d\sigma^{pA \rightarrow \gamma^* \pi^0 X}}{dY_\gamma dY_\pi d^2\mathbf{p}_{\gamma\perp} d^2\mathbf{p}_{\pi\perp} d^2b}}{\iint_{p_{\gamma\perp} > P_{\perp\text{cut}}} d^2\mathbf{p}_{\gamma\perp} \frac{d\sigma^{pA \rightarrow \gamma^* X}}{dY_\gamma d^2\mathbf{p}_{\gamma\perp} d^2b}}, \quad (3)$$

It depends on the angle between the virtual photon and pion, and also on their rapidities. The momentum integrals are manually cut off at a minimum value $p_{\perp\text{cut}}$ to simulate the acceptance of the detector; $p_{\perp\text{cut}}$ can be adjusted to reflect any given experimental apparatus.

This expression (3) can be numerically evaluated for any kinematically allowed values of M , Y_γ , Y_π , $p_{\perp\text{cut}}$, \sqrt{s} , and b , and for any given nuclear gluon distribution $F_{x_g}(q_\perp)$. To evaluate the correlation numerically, we use the MSTW 2008 NLO parton distributions [3] and the DSS fragmentation functions [4].

2.1. Gluon distribution models

For the gluon distribution, we have investigated three models: the GBW model, the BK evolution model with fixed coupling, and BK with running coupling. These are shown in figure 2.

In the GBW model [5], we take the gluon distribution to have an exponential dependence

$$F_{x_g}(k^2, Y) = \frac{1}{\pi Q_{sA}^2(Y)} e^{-k^2/Q_{sA}^2(Y)} \quad (4)$$

where the nuclear saturation scale is given by $Q_{sA}^2 = c(b)A^{1/3}Q_{s0}^2(\frac{x_0}{x})^\lambda$ with $Q_{s0} = 1$ GeV, $x_0 = 0.000304$, and $\lambda = 0.288$.

For the BK model, we use equation (4) at $Y = -\ln 0.01$ as our initial condition and use the BK evolution equation [6, 7] to evolve this to larger values of rapidity. The equation in momentum space is

$$\frac{\partial \phi(k, Y)}{\partial Y} = \bar{\alpha}_s \int_0^\infty \frac{dk'^2}{k'^2} \left[\frac{k'^2 \phi(k') - k^2 \phi(k)}{|k^2 - k'^2|} + \frac{k^2 \phi(k)}{\sqrt{4k'^4 + k^4}} \right] - \bar{\alpha}_s \phi^2(k) \quad (5)$$

F_{x_g} is then computed as the Laplacian of ϕ ,

$F_{x_g}(k^2, Y) = \frac{1}{2\pi k^2} \frac{\partial^2 \phi(k^2, Y)}{\partial (\ln k)^2}$. This model does correctly reproduce the power tail expected from perturbative QCD at large k_\perp , but it disagrees with DIS data: with the standard value of $\alpha_s = 0.2$, the evolution of the saturation scale is too fast.

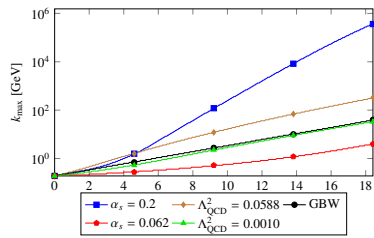


Figure 3: Rapidity dependence of the peak of $k\phi(k)$, which is proportional to the saturation scale, for various parameter choices. Adapted from reference [1].

preference alternative to tuning the fixed coupling. For optimal matching, we do still adjust the value of Λ_{QCD}^2 down from the standard 0.0588 GeV² to 0.001 GeV², and as shown in figure 3, this produces an evolution of the saturation scale very similar to that of the experimentally motivated GBW model.

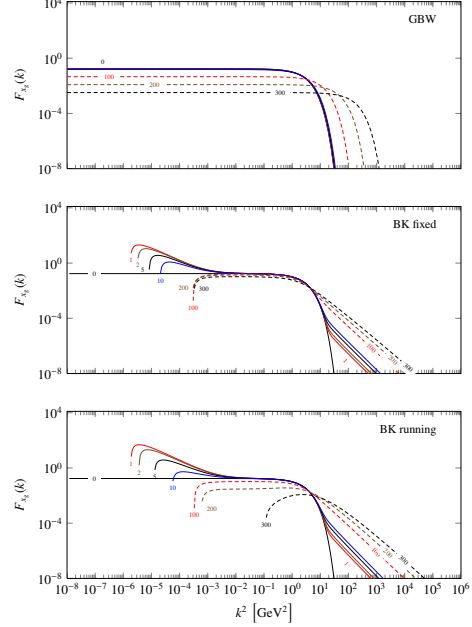


Figure 2: Gluon distributions for the three models. The different curves in each plot correspond to different values of rapidity. Figure adapted from reference [1].

To remedy this, we can slow the evolution of the saturation scale by reducing the value of α_s . Some experimentation shows that $\alpha_s = 0.062$ most closely matches the slope of the saturation scale computed from the GBW model; this is graphically shown in figure 3.

Instead of tuning α_s , we can compute the BK equation with a running coupling, $\bar{\alpha}_s(k^2) = (\beta \ln \frac{k^2 + \mu^2}{\Lambda_{\text{QCD}}^2})^{-1}$. For large rapidities, the saturation scale computed using a running coupling asymptotically scales as $Q_s^2 \sim e^{\lambda_r \sqrt{Y}}$, slower than the fixed-coupling scaling of $Q_s^2 \sim e^{\lambda Y}$. Using a running coupling improves the correspondence with data in other ways as well, so the running coupling may be a physically

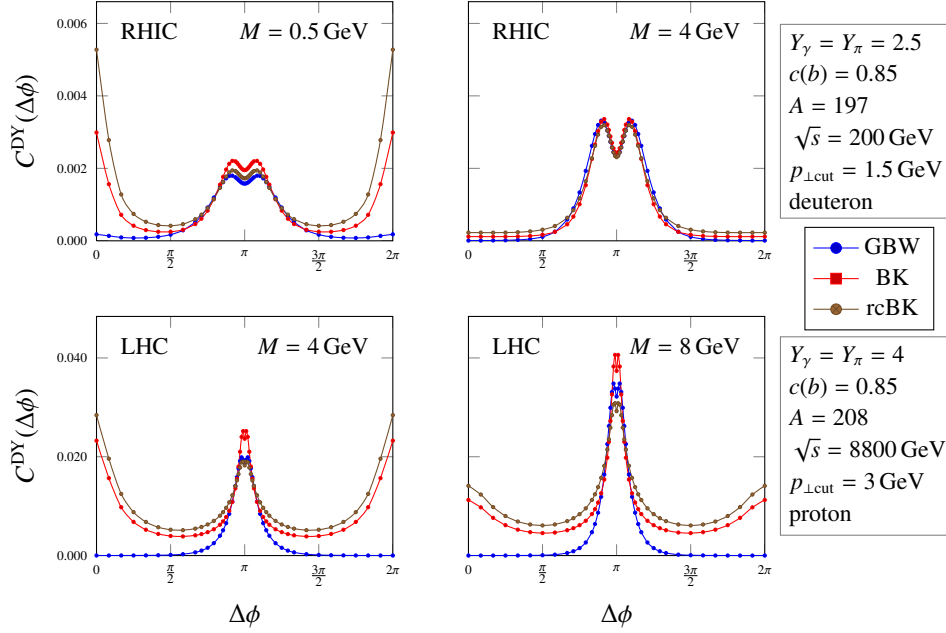


Figure 4: Results of the calculation for parameters corresponding to RHIC (top row) and the LHC at full design energy (bottom row). Plots adapted from reference [1].

3. Results

Given any particular choice of gluon distribution $F_{x_g}(k^2, Y)$, we can calculate numerical values of the correlation from equation (3) by fixing the parameters listed at the right of figure 4. At each collider, we simulate a low-mass and high-mass virtual photon.

A key feature of these results is that the near-side peak around $\Delta\phi = 0$ only appears with the BK equation solution, not the GBW model. The correlation at these angles samples F_{x_g} at large momenta, where the GBW model falls exponentially. We also notice a peculiar double-peak structure around $\Delta\phi = \pi$. This is unique to Drell-Yan processes, and is caused by the parton-level cross section going to zero at a total momentum $q_\perp = 0$. In the higher energy regime the away-side peak is much narrower, and is enhanced in amplitude relative to the near-side peak as compared to the RHIC case.

References

- [1] A. Stasto, B. -W. Xiao and D. Zaslavsky, Phys. Rev. D **86**, 014009 (2012) [arXiv:1204.4861 [hep-ph]].
- [2] F. Dominguez, J. -W. Qiu, B. -W. Xiao and F. Yuan, Phys. Rev. D **85**, 045003 (2012) [arXiv:1109.6293 [hep-ph]].
- [3] A. D. Martin, W. J. Stirling, R. S. Thorne and G. Watt, Eur. Phys. J. C **63**, 189 (2009) [arXiv:0901.0002 [hep-ph]].
- [4] D. de Florian, R. Sassot and M. Stratmann, Phys. Rev. D **75**, 114010 (2007) [arXiv:hep-ph/0703242]; Phys. Rev. D **76**, 074033 (2007) [arXiv:0707.1506 [hep-ph]].
- [5] K. J. Golec-Biernat and M. Wusthoff, Phys. Rev. D **59**, 014017 (1998) [arXiv:hep-ph/9807513].
- [6] I. Balitsky, Nucl. Phys. B **463** (1996) 99 [arXiv:hep-ph/9509348]; Phys. Rev. Lett. **81** (1998) 2024 [arXiv:hep-ph/9807434]; Phys. Lett. B **518** (2001) 235 [arXiv:hep-ph/0105334].
- [7] Y. V. Kovchegov, Phys. Rev. D **60** (1999) 034008 [arXiv:hep-ph/9901281]; Phys. Rev. D **61**, 074018 (2000) [arXiv:hep-ph/9905214].